

# Characterization of alumina:sepiolite monoliths for use as industrial catalyst supports

J. BLANCO, M. YATES\*, P. AVILA, A. BAHAMONDE

*Instituto de Catálisis Y Petroleoquímica (CSIC) Campus de la U.A.M., Cantoblanco 28049 Madrid, Spain*

A series of honeycomb monolithic catalyst supports based on alumina, sepiolite and mixtures of the two were prepared. The textural characterization of these was carried out after heat treatments up to 1473 K, in order to assess the relative merits or drawbacks in the use of sepiolite as a possible admixture to improve the mechanical strengths of the monoliths, whilst preserving high specific surface areas and porosities.

## 1. Introduction

Catalyst supports in a honeycomb configuration generally present advantages over more conventional shapes such as spheres, cylinders etc. in respect to pressure drop and diffusional limitations [1]. However, the low mechanical strength of monoliths based solely on alumina has been a drawback in the utilization of this catalyst support material. Thus the inclusion of binders to improve both the mechanical strength of the finished product and the rheological characteristics during fabrication is essential.

The physical characterization of monoliths prepared from boehmite,  $\alpha$ -sepiolite and mixtures of the two was undertaken. The  $\alpha$ -sepiolite ( $\text{Si}_{12}\text{Mg}_8\text{O}_{30}(\text{OH})_4(\text{H}_2\text{O})_4 \cdot 8\text{H}_2\text{O}$ ) [2], was a natural fibrous mineral ranging from 0.2–2  $\mu\text{m}$  in length and 0.1–0.3  $\mu\text{m}$  [3] in diameter for the bundles of fibres. The choice of  $\alpha$ -sepiolite as a possible admixture was made due to the relatively low cost of the raw material and the enhanced handling characteristics of the paste produced in the early fabrication processes along with the greater mechanical strengths achieved in the finished products [4].

The monoliths were prepared with various alumina:sepiolite compositions and heat treated at temperatures ranging from 773 to 1473 K. The lower temperature was chosen to remove the water of crystallization from the boehmite, lost at *c.* 720 K to give  $\gamma$ -alumina, while the higher temperature was that at which the alumina underwent a phase change to  $\alpha$ -alumina with a consequent reduction in the surface area to a very low level.

## 2. Experimental procedure

### 2.1. Support preparation

The raw materials used were a boehmite (Pural SB  $\text{Al}_2\text{O}_3 \cdot \text{H}_2\text{O}$ ), supplied by Condea, with an average particle size of 90% < 90  $\mu\text{m}$  and a natural  $\alpha$ -sepiolite (Sepiolita-120 NF) supplied by Tolsa S.A., with a

purity of > 80%. Monoliths were prepared to five alumina:sepiolite compositions: 100:0, 80:20, 50:50, 20:80 and 0:100, respectively. The production method used for all of these monoliths outlined below has been reported elsewhere [5].

Samples of the bulk alumina and sepiolite powders were mixed for a minimum of two hours by rotation through the vertical plane at 40 r.p.m. to ensure homogeneity and then added to the kneading machine (WEDA Model AM-3). The required quantity of water was then slowly added and the resulting dough was kneaded for a sufficient period to ensure that a homogeneous mixture of the component materials was obtained.

After kneading, the dough was immediately introduced into the extruder (Cone Drive Transverse City Model SHU-7500C-BJ) and extruded as monoliths of 7.5 channels  $\text{cm}^{-2}$  with a 1 mm wall thickness to *c.* 100 mm lengths. These monoliths were dried at 383 K overnight in an air oven.

The monoliths were heat treated at 773, 1073, 1273 or 1473 K, respectively, in an air atmosphere. The heat treatment for all of the samples followed the same general programme: heated from ambient to the desired temperature at a rate of 2.5  $\text{K min}^{-1}$ , maintained at that temperature for 4 h and then allowed to cool to ambient.

### 2.2. Characterization techniques

Nitrogen adsorption/desorption isotherms at 77 K were determined using a Micromeritics 1310 ASAP. Samples were outgassed overnight at 410 K to a vacuum of <  $10^{-4}$  torr to ensure a dry clean surface, free from any loosely held adsorbed species. Surface area determinations were made by application of the BET equation [6], the linear range of which was usually located between 0.05 and 0.35  $P/P^\circ$ , taking the area of the nitrogen molecule [7] as 0.162  $\text{nm}^2$ . Pore size distribution measurements were made using the BJH method [8] on the desorption isotherm.

\* To whom all correspondence should be addressed.

TABLE I

Alumina: sepiolite ratio	Heat treatment K	N <sub>2</sub> BET area m <sup>2</sup> g <sup>-1</sup>	Hg area m <sup>2</sup> g <sup>-1</sup>	Hg pore volume cm <sup>3</sup> g <sup>-1</sup>	Axial strength Kp mm <sup>-2</sup>
100: 0	773	215.7	110	0.386	1.00
80: 20	773	209.3	79	0.462	0.15
50: 50	773	181.7	73	0.505	1.15
20: 80	773	150.4	72	0.449	1.30
0:100	773	126.3	70	0.502	1.25
100: 0	1073	154.2	166	0.555	1.15
80: 20	1073	147.8	135	0.594	0.25
50: 50	1073	114.6	106	0.575	1.40
20: 80	1073	93.4	81	0.488	1.85
0:100	1073	61.5	69	0.541	1.90
100: 0	1273	103.9	121	0.528	1.20
80: 20	1273	85.6	95	0.524	0.65
50: 50	1273	56.1	64	0.383	3.55
20: 80	1273	32.5	32	0.281	8.60
0:100	1273	8.9	16	0.313	6.60
100: 0	1473	8.6	12	0.362	5.85
80: 20	1473	4.2	7	0.344	0.81
50: 50	1473	1.1	4	0.114	9.20
20: 80	1473	0.6	1	0.015	16.90
0:100	1473	0.1	> 1	0.013	13.90

Mercury intrusion porosimetry (MIP) analyses were performed on a Micromeritics Poresizer 9320 after drying the samples in an oven at 410 K overnight to ensure that the materials were completely dry and the results were thus comparable with those obtained by gas adsorption. Using the nonintersecting cylindrical pore model of Washburn [9] with a mercury contact angle of 140° and surface tension of 480 mN m<sup>-1</sup>, gave a range of *c.* 300 μm–7 nm pore diameter.

Thermal gravimetric analysis (TGA) and differential scanning calorimetry (DSC) determinations were made using a Netzsch STA409EP in an air flow of 75 ml min<sup>-1</sup> with a heating rate of 5 K min<sup>-1</sup> from ambient to 1473 K on samples of *c.* 50 mg.

Powder X-ray diffraction (XRD) patterns were recorded on a Philips PW1710 powder diffractometer in the 3–76° (θ) region using CuK<sub>α</sub> radiation: λ = 0.1518 nm.

The axial strengths of the monoliths were determined using a Chatillon LTCM Universal Tensile Compression and Spring Tester.

The dimensional changes which the monoliths underwent due to heat treatment were determined on representative monolith samples. Their dimensions were measured to an accuracy of 0.01 mm after each heat treatment.

The thermal expansion coefficients (TEC) of samples pretreated at 1200°C were measured using a Netzsch 402EP Dilatometer. Samples of between 25 and 50 mm were heated at 5 K min<sup>-1</sup> from ambient to 1473 K and the expansion measured by the displacement of a strain gauge held against the sample.

### 3. Results and discussion

The specific surface areas (*s*<sub>BET</sub>) of the monoliths from nitrogen adsorption, are presented in column 3 of

Table I. The alumina monolith gave a Type IV isotherm, with a well defined plateau at high relative pressure and narrow hysteresis loop on desorption after treatment at 773 K. This mesoporous character was maintained with heat treatments up to 1273 K, although from the position and shape of the hysteresis curves, shown in Fig. 1, a shift in the pore size distribution to wider pores with increasing pretreatment temperatures was noted.

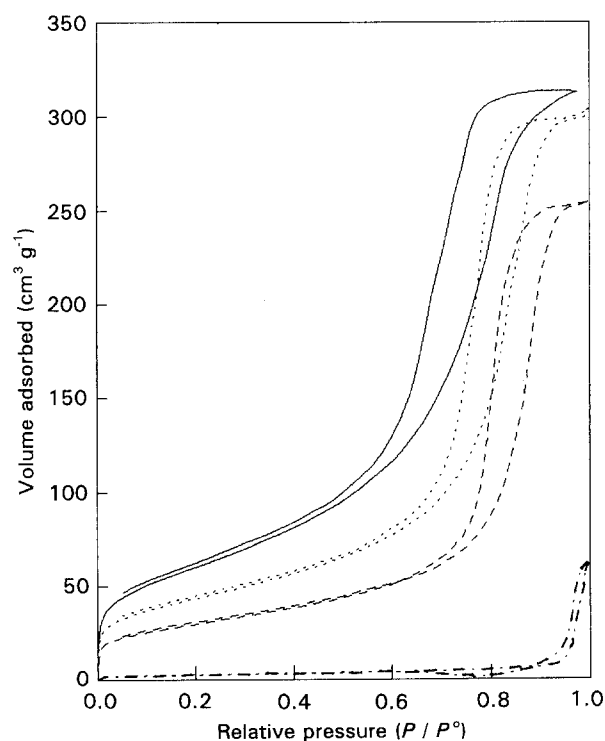


Figure 1 Nitrogen isotherms on heat treated alumina monoliths: — 773 K, --- 1073 K, ···· 1273 K and —·—· 1473 K.

The Type IV character of these materials allowed an accurate assessment of the mesoporosity by converting the volume adsorbed at  $P/P^\circ = 0.95$  on the desorption curve to a liquid volume, assuming the liquid density of nitrogen to be  $0.808 \text{ g cm}^{-3}$ . Thus, at 773, 1073 and 1273 K the calculated mesopore volumes were  $0.48 \text{ cm}^3 \text{ g}^{-1}$ ,  $0.47 \text{ cm}^3 \text{ g}^{-1}$  and  $0.39 \text{ cm}^3 \text{ g}^{-1}$ , respectively. The shifts in the pore size distribution with heat treatments were from 75 nm at 773 K to 84 nm and 101 nm at 1073 and 1273 K, respectively. Treatment at 1473 K caused a collapse of the mesopore structure and reduction of the surface area to a very low level.

The shift to wider mesopores on heat treatments between 773 and 1273 K was thought to be due to partial recrystallization and restructuring within the porous framework of the alumina without disturbing the overall pore geometry. Thus, although the surface areas of the samples were reduced by heat treatments, the mesopore volumes remained relatively stable. The disappearance of the mesopores through heating to 1473 K was due to the transformation of the various alumina species present into a well crystallized  $\alpha$ -alumina phase.

The sepiolite monoliths gave Type II adsorption branches but also displayed hysteresis loops, indicating the presence of mesoporosity which extended into the macropore range, shown in Fig. 2. Although  $\alpha$ -sepiolite was known to possess microporosity in its original state, treatment at 773 K was enough to cause a change in the structure and the original microporosity, formed by the talc ribbons making up the fibres, was no longer available [10]. The absence of microporosity after heat treatment at 773 K or higher was confirmed by using a  $t$ -plot analysis [11], com-

paring the shape of the isotherm with that of a non-porous standard.

The Type II character of the sepiolite prevented an accurate analysis of either the mesopore volume or pore size distribution, although the narrowing of the hysteresis loops were indicative of a general shift to wider pores with increasing heat treatment temperatures in the same manner as that observed with the alumina. The surface areas of these monoliths were also reduced on increasing the pretreatment temperature.

Monoliths of intermediate composition displayed characteristics of the two component materials. The Type II character of the sepiolite dominated the adsorption branch while the mesoporous nature of the alumina tended to widen the hysteresis loop observed on desorption. Due to this mixed shape of the isotherms, accurate assessments of the pore size distributions and pore volumes could not be made.

With increasing heat treatment temperature the surface areas were progressively reduced, until at 1473 K they were very low for all of the samples. The measured surface areas were compared with those calculated for purely physical mixtures of the two component materials (calculated from the surface areas of the pure materials after the same heat treatments). From this analysis, with heat treatments from 773 to 1273 K, the intermediate composition monoliths were found to have surface areas close to those expected, although the 20:80 material was as much as 17% higher than that calculated. However, after treatment at 1473 K the measured surface areas of alumina:sepiolite monoliths were reduced to between *c.* 25–60% of the calculated areas, indicating that a solid state reaction had taken place between the two components, producing a new phase with a substantially lower surface area.

The results from mercury intrusion porosimetry are presented in columns 4 and 5 of Table I. As with the nitrogen adsorption results, the pure samples were taken as standards from which any deviations in the results obtained for the intermediate composition monoliths could be judged. The surface areas, presented in the fourth column of the table, are derived from the intrusion curve using a cylindrical non-intersecting pore model and thus represent the surface area of pores down to 7 nm pore diameter [12].

Discrepancies between the surface area results obtained from both methods were due to the presence of narrow mesopores ( $< 7 \text{ nm}$ ) which remained undetected by the mercury porosimetry technique. Thus, the nitrogen surface areas of samples treated at 773 K were about twice those obtained by mercury intrusion porosimetry. After higher pretreatment temperatures the shifts in the pore size distributions to wider mesopores and eventually to macropores, brought the two measurements of surface area into closer agreement.

The existence of porosity in pores of  $< 7 \text{ nm}$  was also indicated by the shape of the intrusion curves at the highest pressures/smallest pore diameters by a steeply increasing intrusion branch. For both the alumina and sepiolite monoliths this was found to occur up to heat treatments of  $1000^\circ\text{C}$ , and thus under

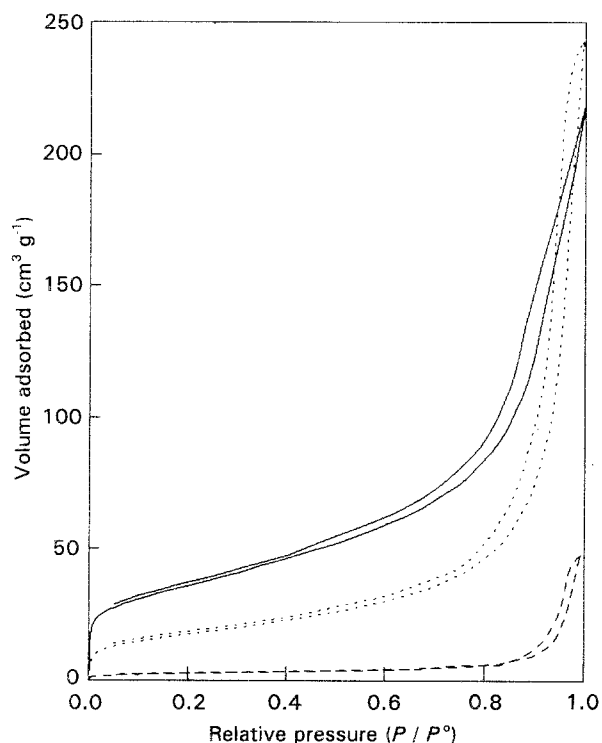


Figure 2 Nitrogen isotherms on heat treated sepiolite monoliths: — 773 K, --- 1073 K and -.- 1273 K.

estimation of the surface area on these and intermediate composition monoliths by the porosimetry technique was to be expected. Similarly, the total pore volumes of the monoliths would be underestimated, and thus, analysis of the results obtained from both methods is necessary for a true estimate of the total pore volume to be made.

The changes in the pore size distributions of the various materials with heat treatments are best appreciated from the intrusion curves shown in Figs 3 and 4 for alumina and sepiolite, respectively. From these figures it should be noted that, in general, increases in the heat treatment temperature lead to a shift in the pore size distribution to wider pores and a reduction in the cumulative pore volume. Although the total pore volumes of materials treated at 773 K were lower than those treated at 1073 K, this was due to the underestimation of the true pore volumes of these materials which possessed a substantial fraction of their porosities in pores of less than 7 nm. The shifts in the pore size distributions in the mesopore range were in agreement with those observed from the gas adsorption results.

Using a similar analysis procedure to that employed with gas adsorption, the measured total pore volumes

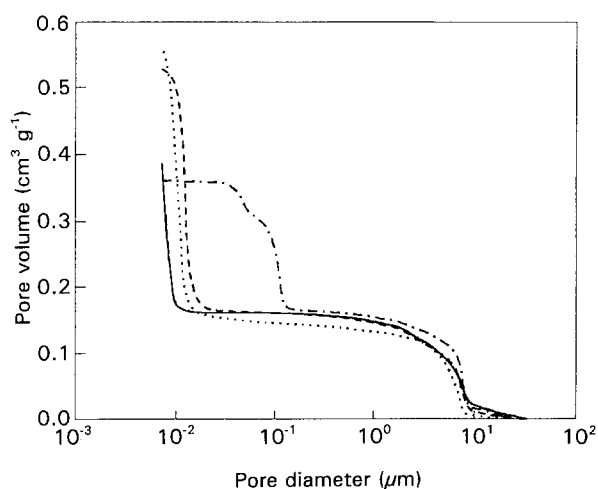


Figure 3 MIP curves on heat treated alumina monoliths: — 773 K, ... 1073 K, --- 1273 K and - - - 1473 K.

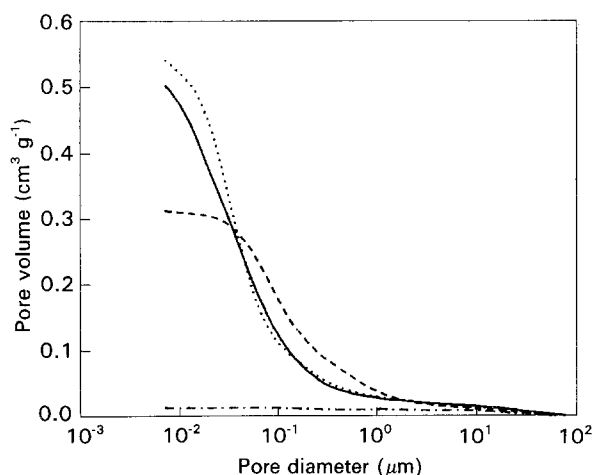


Figure 4 MIP curves on heat treated sepiolite monoliths: — 773 K, ... 1073 K, --- 1273 K and - - - 1473 K.

were compared with those calculated for purely physical mixtures of the alumina and sepiolite. At 773 K an increase in the pore volumes of the 80:20 and 50:50 samples was noted while a slight reduction for the 20:80 material was observed. At 1073 K the 20:80 material displayed a further reduction whilst the other two gave the expected results. With treatment at 1273 K the pore volume of the 80:20 material was slightly higher than the calculated value while the other two were lower than expected, especially the 20:80 sample. This trend was repeated at 1473 K but with much greater differences between the measured and calculated results.

With heat treatments up to 1273 K the shapes of the intrusion curves were generally those expected for purely physical mixtures of the types of porosity present due to the alumina and sepiolite. However, after treatment at 1473 K the shape of the intrusion curve bore no relation to that observed with either sepiolite or alumina, Fig. 5. This latter result was strongly indicative of a solid state reaction having taken place between alumina and sepiolite at this temperature.

The results of the fracture strength testing are presented in the final column of Table I. Of note was the increase in overall strength brought about through pretreatment at successively higher temperatures. This was in part due to the reduction in the total porosities of the monoliths with increasing temperature. Since the measured crushing strength of a brittle ceramic body is inversely proportional to its overall porosity [13], an increase in strength was to be expected with the decreases in porosity observed from mercury intrusion porosimetry.

The axial crushing strengths of the alumina monoliths were not significantly increased until after treatment at 1473 K. This was in agreement with the results obtained by nitrogen adsorption and mercury intrusion porosimetry which demonstrated the stability of the mesopore volume up to 1273 K, which limited the strength development.

The sepiolite monoliths displayed a steady progression in strength development with increasing heat treatment, as expected from the observed reductions

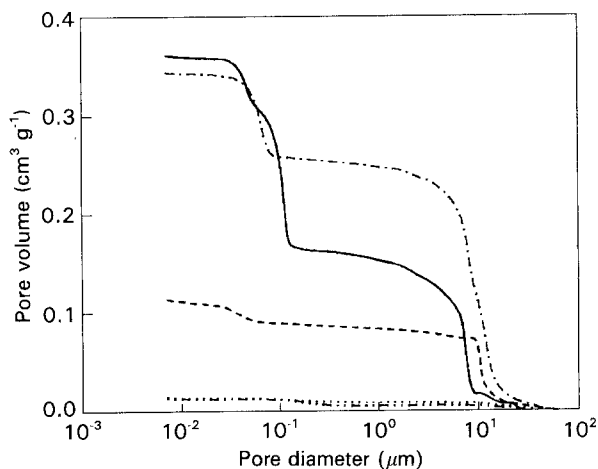


Figure 5 MIP curves on alumina: sepiolite monoliths heat treated at 1473 K. Ratio: — 100:0, - - - 80:20, ... 50:50, - · - · 20:80 and - - - 0:100.

in the porosities of these materials. For the intermediate composition monoliths the strengths were found to be lower than expected in alumina-rich materials but higher than calculated in sepiolite-rich materials, especially after treatment at 1273 and 1473 K.

The axial crushing strength of the 20:80 material treated at 1473 K was approximately three times that of the alumina monolith, while the 80:20 material showed a reduced strength compared to that of the alumina monolith. These results were in agreement with the observed porosities, where the increased pore volume of the 80:20 material led to the decrease in strength, while the reduced pore volume of the 20:80 sample gave rise to the improvement in strength. The relationship between strength and pore volume after treatment at 1473 K is shown from the results presented in Fig. 6.

TGA/DSC measurements were determined on the alumina and sepiolite samples. For the alumina an initial weight loss of *c.* 7% with a maximum in the DSC curve at 350 K, associated with loss of adsorbed water, was observed. A second weight loss of *c.* 16%, due to loss of the water of crystallization from the boehmite starting material to form  $\gamma$ -alumina, was centred around 710 K. Above this temperature no further weight losses were observed although inflections in the DSC curve were indicative of the phase changes which culminated in the formation of  $\alpha$ -alumina at 1473 K.

The sepiolite monolith showed an initial weight loss of *c.* 8% with a maximum in the DSC curve close to 350 K due to loss of physisorbed water. An endotherm between 570–620 K was produced by loss of zeolitic water and water of crystallization, associated with the collapse of the internal structure to produce anhydrous sepiolite [14]. At this point the material may be rehydrated back to its original state. Heating between

670–870 K caused the loss of constitutional water and the material could no longer be rehydrated [15]. Between 870–970 K a further weight loss was produced, thought to be due to loss of water present as hydroxyl groups. A very well defined exothermic peak at *c.* 1100 K due to the phase change to enstatite was observed although no further weight losses were recorded.

Powder (XRD) studies on ground samples of the monoliths were determined to follow any phase changes and solid state reactions which resulted from heating the materials to 1473 K. It should be noted that for crystalline phases to be detected by XRD the crystallites must be greater than 3 nm. Thus, the presence of certain phases may not be detected due to the small size of the crystallites which would appear amorphous.

Between 773 and 1273 K the alumina monoliths gave rise to largely amorphous XRD patterns although the presence of several forms of alumina ( $\beta$ ,  $\gamma$ ,  $\delta$ ,  $\epsilon$ ) were indicated by poorly defined peaks within the spectra. Treatment at 1473 K produced a well crystallized  $\alpha$ -alumina. The XRD patterns obtained from the sepiolite monoliths under the same conditions gave the expected peaks for sepiolite after heat treatment at 773 and 1073 K, and thereafter the peaks for enstatite as the sepiolite underwent a phase change on heat treatments higher than 1100 K.

Powder XRD patterns of the mixed composition monoliths displayed interesting differences to those obtained with the two raw materials due to solid state reactions between the alumina and sepiolite. At all compositions and all temperatures the presence of spinel ( $\text{MgO} \cdot \text{Al}_2\text{O}_3$ ) was noted due to the reaction between alumina and the readily accessible magnesia present at the surface of the sepiolite. A further new phase, noted only after treatment at 1473 K, was that of cordierite ( $2\text{MgO} \cdot 2\text{Al}_2\text{O}_3 \cdot 5\text{SiO}_2$ ). The formation of this phase along with the spinel caused the complete absence of peaks due to  $\alpha$ -alumina in 20:80 compositions treated at 1473 K, suggesting that all of the alumina had undergone solid state reactions to form these two phases. The curves depicting the phases present after heat treatment at 1473 K in relation to the initial alumina:sepiolite ratio are shown in Fig. 7.

The TEC of a monolithic support is an important aspect in determining its usefulness in practice since large volume changes under the usual working temperature range of the catalysts are undesirable. Determination of this property required that the measurement was that of a purely reversible thermal expansion and did not contain any elements due to loss of free and bound water, hydroxyl groups or any phase changes and solid state reactions. Thus, the TECs, shown in Fig. 8, were measured on samples which had been previously heated to 1473 K for 4 h. All monoliths of mixed compositions had lower TECs than those measured for alumina or sepiolite with the lowest values found with compositions of between 30–50% alumina.

The dimensional changes which the monoliths underwent on heat treatment were determined in all three planes: horizontally and vertically across the

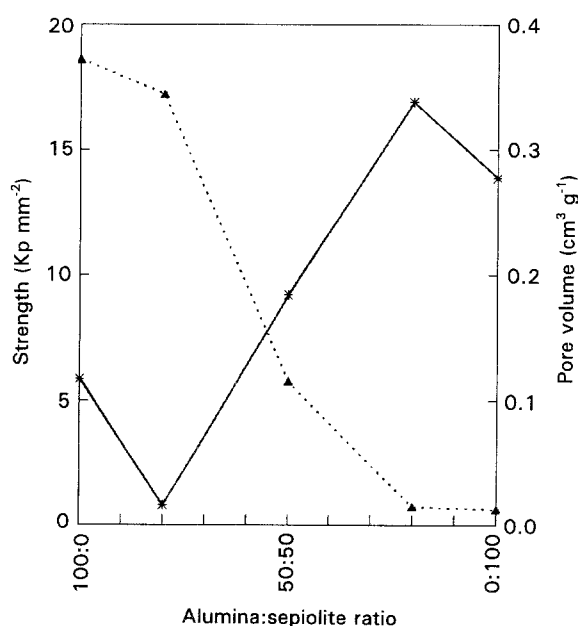


Figure 6 Relationship between axial strength and pore volume of alumina:sepiolite monoliths heat treated at 1473 K: —\*— strength and  $\cdot \blacktriangle \cdot$  pore volume.

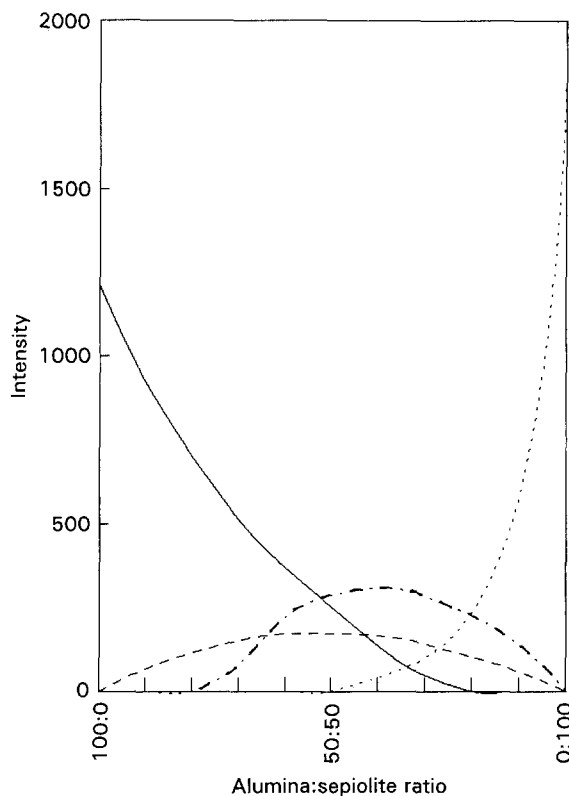


Figure 7 XRD analysis of alumina:sepiolite monoliths heat treated at 1473 K: — alumina, ··· enstatite, --- spinel and -·-· cordierite.

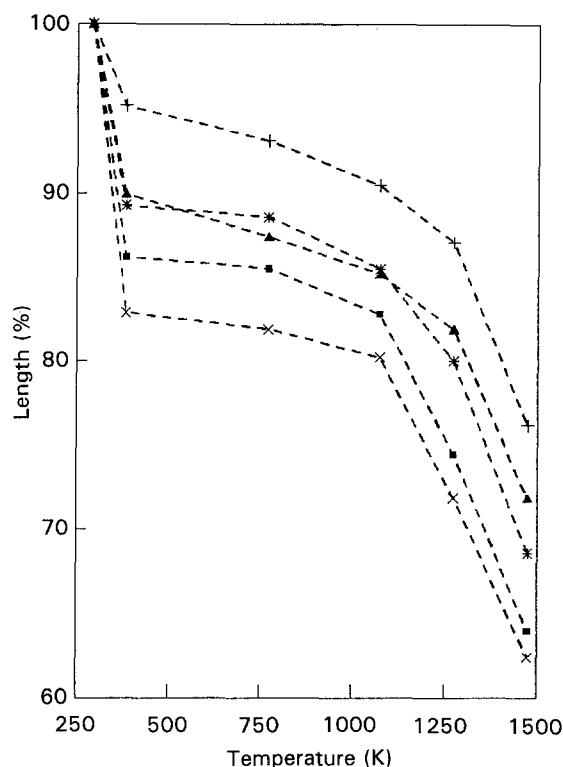


Figure 9 Length changes of alumina:sepiolite monoliths with heat treatment. Ratio: —▲— 100:0, ·+· 80:20, —\*— 50:50, —■— 20:80 and ·×· 0:100.

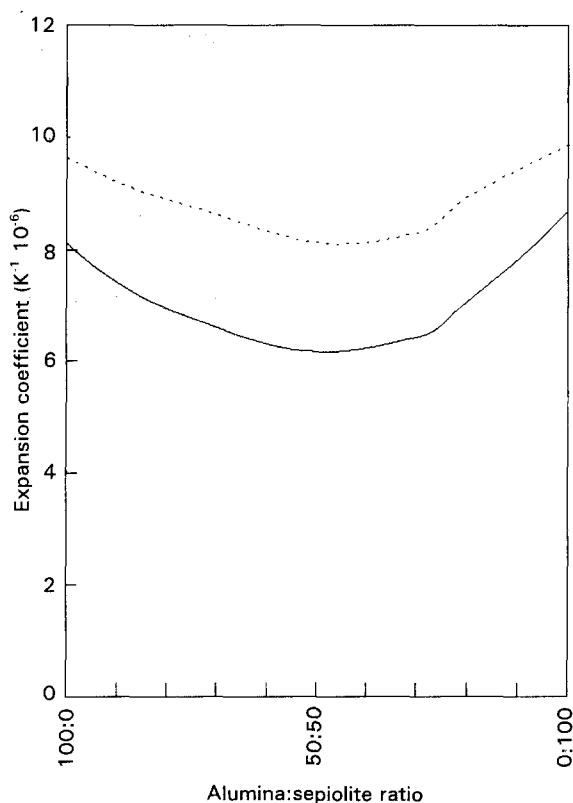


Figure 8 TECs of alumina:sepiolite monoliths heat treated at 1473 K: range — 25–800°C and ... 300–1100°C.

face of the monolith and along its length, respectively. The percentage length changes due to heat treatments were found to be the same along each axis. Although all of the materials underwent the same general trends

with heat treatment, there were marked differences in the magnitude of the changes observed depending on the initial compositions of the monoliths.

Curves of the percentage length changes versus heat treatment are presented in Fig. 9. The shrinkage observed on heating from ambient to 380 K was due to the loss of water from the structure, allowing the solid phases to come closer together. Since the samples had all been initially produced as monoliths from a dough which included water, in order to achieve a workable paste, this had invariably led to the incorporation of water into the structure which was not chemically bound and thus easily eliminated on heating to 380 K. After the shrinkage due to the loss of free water the monoliths displayed a long interval of relative dimensional stability up to 1073 K. A further shrinkage was observed on heat treatments between 1073 and 1473 K.

The order of the dimensional changes were of note since they could be related, in general terms, to the axial strengths of the materials. Thus, the sepiolite monolith, which was much stronger than the corresponding alumina material, showed the greatest shrinkage on heat treatment. The 80:20 sample had the highest dimensional stability, which was in agreement with its poor axial strength. Similarly, the sepiolite rich 20:80 material underwent severe shrinkage with heat treatment and consequently showed a greatly improved strength.

The monoliths based solely on sepiolite exhibited greater shrinkage at all heat treatments than the corresponding 20:80 material, but their axial strengths were less, even though the pore volumes were similar, due to the presence of wider pores. This de-

pendence of the axial strength on the pore width as well as the pore volume was further illustrated by the results obtained with the 80:20 sample after heat treatment at 1473 K.

#### 4. Conclusions

1. Through the correct choice of monolith composition and thermal treatment a substantial enhancement in the mechanical strength could be achieved while maintaining desirably high values of surface area and porosity depending on the intended utilization of the monolith.

2. For low and medium sepiolite contents the monoliths displayed pore size distributions characteristic of the corresponding physical mixtures. However, at higher sepiolite loadings a reduction in the pore volume was accompanied by a three-fold increase in the mechanical strength, in comparison to that of the pure alumina monolith.

3. The behaviour of the monoliths after treatment at 1473 K was dominated by the solid state reactions between the alumina and sepiolite. The XRD results confirmed the formation of a phase attributable to spinel at all temperatures, but with the major change occurring at 1473 K with the formation of cordierite.

4. The results demonstrate the beneficial nature of the inclusion of sepiolite in the reduction of the TECs of the monoliths, with the lowest values found for materials with an initial sepiolite composition lying between 50–70%.

#### References

1. R. K. SHAH and A. L. LONDON, *Tech. Rep. 75* (1971) Dept. Mech. Eng. Stanford University CA.
2. K. BRUNAUER and A. PREISINGER, *Tschermaks Miner. Petr. Mitt.* **6** (1956) 120.
3. A. ALVAREZ, in "Developments in Sedimentology" **37**, edited by A. Singer & E. Galan (Elsevier, 1984) p. 253.
4. P. AVILA, J. BLANCO, A. BAHAMONDE, J. M. PALACIOS and C. BARTHELEMY, *J. Mater. Sci.* **28** (1993) 4113.
5. A. BAHAMONDE, PhD thesis, Universidad Complutense, Madrid (1992).
6. S. BRUNAUER, P. H. EMMETT and E. TELLER, *J. Amer. Chem. Soc.* **60** (1938) 309.
7. K. S. W. SING, D. H. EVERETT, R. A. W. HAUL, L. MOSCOU, R. A. PIEROTI, J. ROUQUEROL and T. SIEMIENIEWSKA, *Pure and Appl. Chem.* **57** (1985) 4, 603.
8. E. P. BARRETT, L. G. JOYNER and P. H. HALENDA, *J. Amer. Chem. Soc.* **73** (1951) 373.
9. E. W. WASHBURN, *Proc. Nat. Acad. Sci. USA* **7** (1921) 115.
10. Y. GRILLET, J. M. CASES, M. FRANCOIS, J. ROUQUEROL and J. E. POIRIER, *Clay Miner.* **36** (1988) 233.
11. J. H. DE BOER, J. H. LIPPENS, B. G. LINSEN, J. C. P. BROEKHOFF, A. VAN DEN HEUWAL and TH. J. OSINGA, *J. Colloid Interface Sci.* **21** (1966) 405.
12. H. M. ROOTARE and C. F. PRENZLOW, *J. Phys. Chem.* **71** (1967) 2733.
13. G. VEKINIS, M. F. ASHBY and P. W. R. BEAUMENT, *J. Mater. Sci.* **28** (1993) 3221.
14. A. PREISINGER, *Clay Miner.* **6** (1959) 61.
15. T. FERNANDEZ ALVAREZ, in Proceedings Reunion Hispano-Belga Minerales y Arcillas, Edited by J. M. Serotosa (Consejo Superior de Investigaciones Cientificas, Madrid, 1970) p. 202.

*Received 5 August 1993  
and accepted 21 March 1994*